

---

# HyMARC Seedling: Super Metalated Frameworks as Hydrogen Sponges

Omar M. Yaghi (Primary Contact),  
Bunyarat Rungtaweivoranit, Roc Matheu,  
Robinson W. Flaig, Nikita Hanikel, Sophia Steffens  
University of California, Berkeley  
Department of Chemistry  
419 Latimer Hall  
Berkeley, California 94720  
Phone: (510) 643-5507  
Email: [yaghi@berkeley.edu](mailto:yaghi@berkeley.edu)

DOE Manager: Jesse Adams  
Phone: (720) 356-1421  
Email: [Jesse.Adams@ee.doe.gov](mailto:Jesse.Adams@ee.doe.gov)

Contract Number: DE-EE0008094

Project Start Date: September 1, 2017  
Project End Date: August 31, 2018

## Overall Objectives

- Introduce a large number of open metal sites into metal-organic frameworks (MOFs) to achieve improved hydrogen storage under ambient conditions.
- Install metal complexes in the pores of MOFs by post-synthetic modification (PSM) to produce super metalated MOFs that contain a high density of open metal sites with enhanced affinity for hydrogen molecules.
- At least double the state-of-the-art open metal site density in MOFs and thus produce hydrogen adsorbents with capacity exceeding the 2025 DOE system targets of 40 g/L and 5.5 wt% under ambient conditions.

## Fiscal Year (FY) 2018 Objectives

- Synthesize crystalline functionalized IRMOF-74 series.
- Characterize IRMOF-74 backbones after PSM to quantify pore volumes and amount of metal binding sites.
- Characterize the as-synthesized super metalated frameworks to quantify metal incorporation.

- Develop a MOF with (1) double the amount of open metal sites compared to the unfunctionalized IRMOF-74 backbone before PSM and (2) total volumetric capacity of 18 g/L H<sub>2</sub> at 20°C and less than 100 bar based on single-crystal density.

## Technical Barriers

This project addresses the following technical barriers from the Hydrogen Storage section of the Fuel Cell Technologies Office Multi-Year Research, Development, and Demonstration Plan<sup>1</sup>:

- (C) Efficiency
- (D) Durability/Operability
- (E) Charging/Discharging Rates.

## Technical Targets

The objective of this project is to introduce a large number of open metal sites into MOFs to achieve improved hydrogen storage under ambient conditions. Insights gained from these studies will be applied toward the design and synthesis of hydrogen storage materials that meet the following 2025 DOE hydrogen storage targets:

- Gravimetric capacity: 0.055 kg H<sub>2</sub>/kg system
- Volumetric capacity: 0.040 kg H<sub>2</sub>/L system
- Operating ambient temperature: -40°/60°C
- Operational cycle life (1/4 tank to full): 1,500 cycles
- Onboard efficiency: 90%
- System fill time (5 kg): 3–5 mins
- Minimum full flow rate: 0.02 (g/s)/kW

## FY 2018 Accomplishments

- Crystalline, porous (BET SA: ~1800 m<sup>2</sup> g<sup>-1</sup>) Mg-IRMOF-74-III-(CH<sub>2</sub>NH<sub>2</sub>)<sub>2</sub> was synthesized.

---

<sup>1</sup> <https://www.energy.gov/eere/fuelcells/downloads/fuel-cell-technologies-office-multi-year-research-development-and-22>

- The primary amines of the MOF were reacted with 2-hydroxybenzaldehyde to produce Mg-IRMOF-74-2OHBAL and with 3,4-dihydroxybenzaldehyde to give Mg-IRMOF-74-34OHBAL. Both reactions proceeded with quantitative yields.
- Post-synthetically modified MOFs were decorated with Ni complexes with approximately 45% yield.
- Attempts were made to activate the framework materials to liberate open metal sites.
- At 77 K, these materials exhibited gravimetric hydrogen uptake capacities of 0.923 wt%.

## INTRODUCTION

MOFs possess many desirable attributes allowing for enhanced hydrogen storage. They are highly porous and systematically tunable or functionalizable [1]. Extensive studies regarding the hydrogen adsorption properties of MOFs have shown that MOFs are promising candidates as sorbent materials. There is the potential for MOFs to reach the DOE target for gravimetric hydrogen uptake, albeit at 77 K [2]. A linear correlation between gravimetric uptake and surface area at this temperature and high pressure (1–26 bar) has been observed and noted [3]. However, at typical operating temperatures (e.g., 298 K), MOFs' gravimetric hydrogen uptakes decrease dramatically due to the characteristically weak interactions between hydrogen adsorbate molecules and the frameworks [4]. To augment the strength of such interactions, several strategies have been developed including catenation and adsorption on open metal sites [5]. Of these parameters, an increase in the density of cationic open metal sites effectively enhances frameworks' interactions with hydrogen adsorbate molecules. After solvothermal MOF synthesis, solvent molecules remain and serve as capping ligands on the metal clusters. These can be removed upon evacuation to create coordinatively unsaturated open metal sites [6]. Open metal sites interact with hydrogen through charge-induced dipole interaction, greatly increasing isosteric heats of adsorption [7]. Among MOFs that apply this interaction, Ni<sub>2</sub>(*m*-dobdc), a MOF-74 analogue, exhibits the highest observed volumetric hydrogen uptake (12.1 g L<sup>-1</sup> at 25°C and 100 bar) with adsorption enthalpy of up to 13.7 kJ mol<sup>-1</sup> at zero coverage [8]. However, these values remain below the DOE 2025 targets for hydrogen storage (40 g L<sup>-1</sup>), prompting further investigation.

## APPROACH

In this work, Mg-IRMOF-74-III was chosen as a platform for introducing additional open metal sites due to its high surface area, chemical tunability, stability, and availability of open metal sites that can interact with hydrogen molecules [9,10]. The organic linker of this MOF was functionalized with primary amines that were post-synthetically modified (PSM) to install metal-binding ligands for subsequent metalations [11] (Figure 1). The resultant materials were investigated for hydrogen adsorption properties and capacities.

Imine condensation was selected as a method of post-synthetic ligand installation in the MOF. This class of reactions can proceed under mild conditions with high yield. Additionally, no sterically bulky leaving group is involved in the process, allowing the reactions to occur without negative impacts from poor reactant and product diffusion [12]. In this work, the primary amines of the MOF were reacted with 2-hydroxybenzaldehyde to produce Mg-IRMOF-74-2OHBAL and with 3,4-dihydroxybenzaldehyde to give Mg-IRMOF-74-34OHBAL. These two ligands were selected based on their ability to bind to a wide variety of metals, including nickel [13,14]. Additionally, the catecholate functionality in Mg-IRMOF-74-34OHBAL can benefit hydrogen storage based on the fact that this ligand is capable of polarizing molecules such as hydrogen [15]. These MOFs were subsequently metalated with Ni(II) salts. Open metal sites of Ni(II) have the highest hydrogen adsorption enthalpies among many divalent metals [7]. Activation conditions for the resultant metalated frameworks were screened and hydrogen sorption isotherms were measured at 77 K to assess the frameworks' storage capacities.

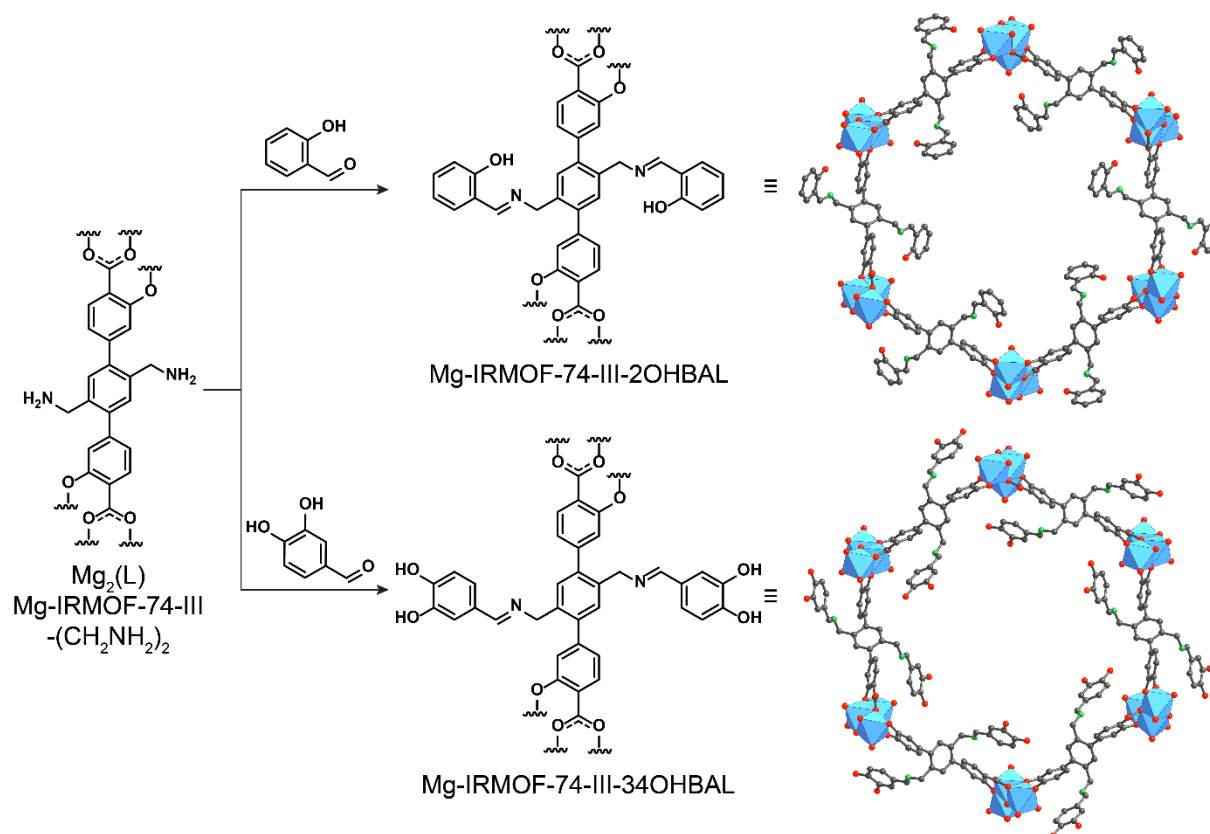


Figure 1. Post-synthetic modifications of Mg-IRMOF-74-III-(CH<sub>2</sub>NH<sub>2</sub>)<sub>2</sub> with 2-hydroxybenzaldehyde and 3,4-dihydroxybenzaldehyde to produce Mg-IRMOF-74-III-2OHBAL and Mg-IRMOF-74-III-34OHBAL, respectively

## RESULTS

Mg-MOF-74 was synthesized with slight modifications from the reported procedure [16] in a 20-mL scintillation vial with Mg(NO<sub>3</sub>)<sub>2</sub>·6H<sub>2</sub>O (116 mg, 0.450 mmol) and 2,5-dihydroxy-1,4-benzenedicarboxylic acid (30 mg, 0.151 mmol). The reaction was heated in a 120°C isothermal oven for a day. Yellow microcrystalline powder was washed with DMF five times (10 mL × 5) over a 48-h period and with anhydrous methanol five times (10 mL × 5) over a 48-h period.

Mg-IRMOF-74-III-(CH<sub>2</sub>NH<sub>2</sub>)<sub>2</sub> was synthesized according to the reported procedure [11]. The resulting pale-yellow powder (~100 mg) was washed with DMF three times (10 mL × 3) over a 24-h period and with ethyl acetate three times (10 mL × 3) over a 24-h period.

Mg-IRMOF-74-III-(CH<sub>2</sub>NH<sub>2</sub>)<sub>2</sub>-2OHBAL was synthesized by PSM of Mg-IRMOF-74-III-(CH<sub>2</sub>NH<sub>2</sub>)<sub>2</sub>. In a 20-mL scintillation vial, Mg-IRMOF-74-III-(CH<sub>2</sub>NH<sub>2</sub>)<sub>2</sub> was added to a solution of 2-hydroxybenzaldehyde (537 mg) dissolved in ethyl acetate (5 mL). The suspension was allowed to react at room temperature for 18 h. The resultant orange powder was washed with ethyl acetate five times (20 mL × 5) over a 48-h period. In preparation for material characterization, the sample was dried under vacuum at 120°C for 6 h.

Mg-IRMOF-74-III-(CH<sub>2</sub>NH<sub>2</sub>)<sub>2</sub>-34OHBAL was synthesized by post-synthetic modification of Mg-IRMOF-74-III-(CH<sub>2</sub>NH<sub>2</sub>)<sub>2</sub>. In a 20-mL scintillation vial, Mg-IRMOF-74-III-(CH<sub>2</sub>NH<sub>2</sub>)<sub>2</sub> was added to a solution of 3,4-dihydroxybenzaldehyde (607 mg) dissolved in ethyl acetate (20 mL). The suspension was allowed to react at room temperature for 18 h. The resultant red powder was washed with ethyl acetate five times (20 mL × 5) over a 48-h period. In preparation for material characterization, the sample was dried under vacuum at 120°C for 6 h.

To metalate Mg-IRMOF-74-III-(CH<sub>2</sub>NH<sub>2</sub>)<sub>2</sub>-2OHBAL, yielding Mg-IRMOF-74-III-(CH<sub>2</sub>NH<sub>2</sub>)<sub>2</sub>-2OHBAL-Ni, Mg-IRMOF-74-III-(CH<sub>2</sub>NH<sub>2</sub>)<sub>2</sub>-2OHBAL (~30 mg) was washed with anhydrous MeOH three times (20 mL × 3). The MOF was added to a solution of Ni(OAc)<sub>2</sub>·4H<sub>2</sub>O (197 mg) dissolved in anhydrous MeOH (6 mL). The suspension was allowed to react at room temperature for 7 days. The resultant yellow powder was washed with anhydrous MeOH five times (10 mL × 5) over a 48-h period.

To metalate Mg-IRMOF-74-III-(CH<sub>2</sub>NH<sub>2</sub>)<sub>2</sub>-34OHBAL, yielding Mg-IRMOF-74-III-(CH<sub>2</sub>NH<sub>2</sub>)<sub>2</sub>-34OHBAL-Ni, Mg-IRMOF-74-III-(CH<sub>2</sub>NH<sub>2</sub>)<sub>2</sub>-34OHBAL (~30 mg) was washed with anhydrous MeOH three times (20 mL × 3). The MOF was added to a solution of Ni(OAc)<sub>2</sub>·4H<sub>2</sub>O (197 mg) dissolved in anhydrous MeOH (6 mL). The suspension was allowed to react at room temperature for 7 days. The resultant red powder was washed with anhydrous MeOH five times (10 mL × 5) over a 48-h period.

Powder X-ray diffraction (PXRD) analysis indicates that the materials retain crystallinity and phase purity after PSM (Figure 2a). Nitrogen adsorption isotherms performed at 77 K indicate that these materials remain porous after these processes as well (Brunauer-Emmett-Teller surface area of Mg-IRMOF-74-III-(CH<sub>2</sub>NH<sub>2</sub>)<sub>2</sub> = 1,840 m<sup>2</sup> g<sup>-1</sup>, Mg-IRMOF-74-2OHBAL = 840 m<sup>2</sup> g<sup>-1</sup>, and Mg-IRMOF-74-34OHBAL = 905 m<sup>2</sup> g<sup>-1</sup>) (Figure 2b). MOF powders were digested in DCI/DMSO-*d*<sub>6</sub> to determine the yield of the imine condensation reactions in these MOFs, demonstrating quantitative yields in reactions between the linker-based primary amines with both aldehyde derivatives. Due to imine bonds' sensitivities to acid, only hydrolyzed products were observed from <sup>1</sup>H-NMR analysis of digested MOF samples. To confirm the presence of imine bonds in both materials, Fourier transform infrared spectroscopy (FT-IR) was performed. The results indicated the presence of imine stretches at 1,629 and 1,639 cm<sup>-1</sup> for -2OHBAL and -34OHBAL adducts, respectively (Figure 3). These characteristic imine stretches were corroborated by the spectra obtained from molecular model compounds.

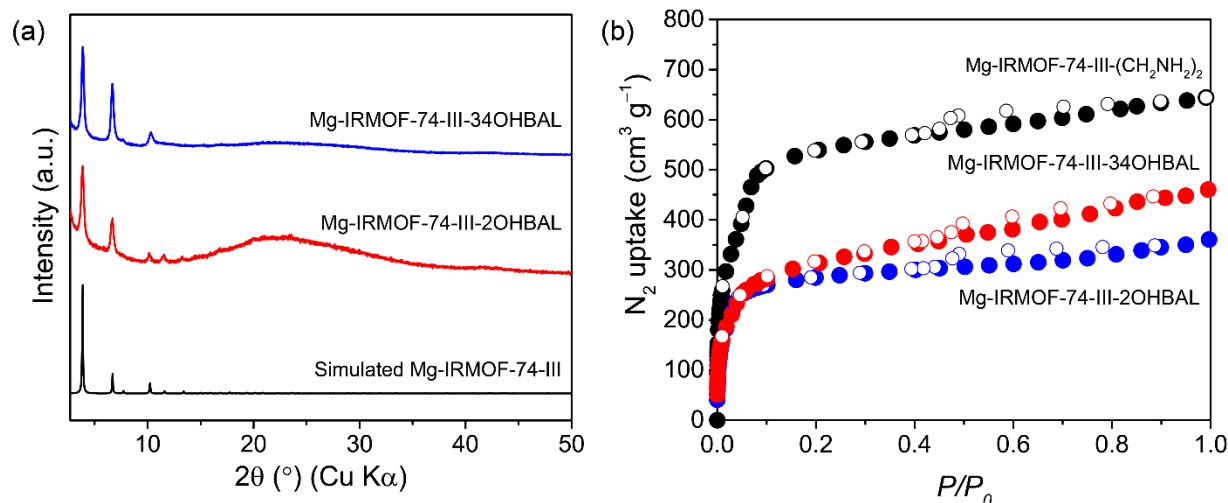
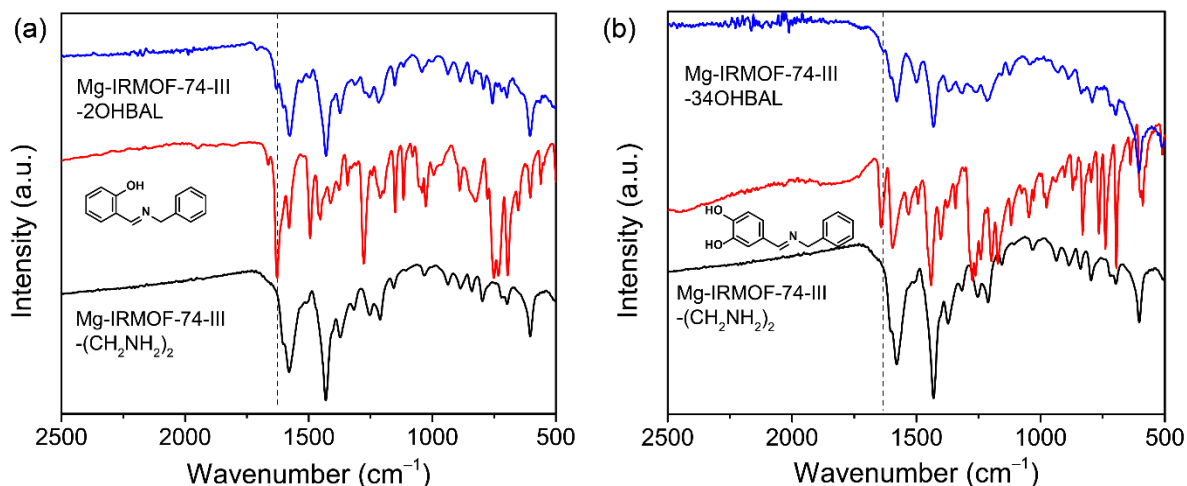


Figure 2. (a) Experimental PXRD patterns of functionalized Mg-IRMOF-74-III-(CH<sub>2</sub>NH<sub>2</sub>)<sub>2</sub> in comparison with simulated patterns of Mg-IRMOF-74-III-(CH<sub>2</sub>NH<sub>2</sub>)<sub>2</sub> and (b) nitrogen adsorption-desorption isotherms at 77 K with adsorption and desorption points represented by closed circles and open circles, respectively ( $P/P_0$ , relative pressure)



**Figure 3.** FT-IR spectra of Mg-IRMOF-74-III-2OHBAL and Mg-IRMOF-74-III-34OHBAL in comparison with their respective model compounds

In the metalation process, reaction conditions were optimized via screening of reaction times between 1 and 7 days and Ni salts including  $\text{Ni}(\text{OAc})_2 \cdot 4\text{H}_2\text{O}$ ,  $\text{NiCl}_2 \cdot \text{glyme}$  and  $\text{Ni}(\text{NO}_3)_2 \cdot 6\text{H}_2\text{O}$ . For Mg-IRMOF-74-2OHBAL, only Ni(II) from  $\text{Ni}(\text{OAc})_2 \cdot 4\text{H}_2\text{O}$  successfully incorporated into the MOF structure as indicated by inductively coupled plasma analysis. This analysis indicated that the Ni/Mg molar ratio was 0.43, or a 43% metalation yield of the available ligands. Interestingly, Mg-IRMOF-74-III-34OHBAL can be metalated with all Ni(II) salts tested including  $\text{Ni}(\text{OAc})_2 \cdot 4\text{H}_2\text{O}$ ,  $\text{NiCl}_2 \cdot \text{glyme}$  and  $\text{Ni}(\text{NO}_3)_2 \cdot 6\text{H}_2\text{O}$  to give Ni/Mg molar ratios of 0.44, 0.22, and 0.33, respectively. As a control experiment, Mg-MOF-74, which is a Mg-IRMOF-74-III analog with 2,5-dioxido-1,4-benzenedicarboxylate as organic linker, was synthesized and tested for metalation under similar conditions. Negligible incorporation of Ni(II) was found confirming that Ni(II) was bound to the ligands in Mg-IRMOF-74-2OHBAL and Mg-IRMOF-74-34OHBAL. Additionally, we performed X-ray photoelectron spectroscopy (XPS) of metalated samples to probe the change in the electronic properties of Ni(II) after metalation. High-resolution Ni 2p XPS spectra of these samples show two regions assigned as Ni(II)  $2p_{3/2}$  and satellites (Figure 4) [17].  $\text{Ni}(\text{OAc})_2 \cdot 4\text{H}_2\text{O}$ , Mg-IRMOF-74-2OHBAL-Ni and Mg-IRMOF-74-34OHBAL-Ni (metalated with  $\text{Ni}(\text{OAc})_2 \cdot 4\text{H}_2\text{O}$ ) exhibit binding energies of 856.2, 855.8, and 855.9 eV, respectively. The decreased binding energies after metalation indicate the increase in the electron donor ability of the ligands appended to the MOF [18]. PXRD analysis indicates that these materials remain crystalline and FT-IR spectra shows that imine bonds remain intact.

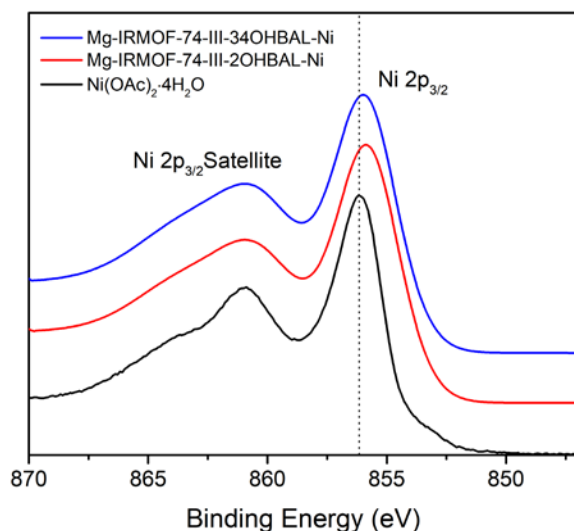


Figure 4. XPS Ni  $2p_{3/2}$  spectra of Mg-IRMOF-74-III-( $\text{CH}_2\text{NH}_2$ )<sub>2</sub>-2OHBAL-Ni and Mg-IRMOF-74-III-( $\text{CH}_2\text{NH}_2$ )<sub>2</sub>-34OHBAL-Ni in comparison with the Ni(II) precursor, which is Ni(OAc)<sub>2</sub>·4H<sub>2</sub>O

Low-pressure hydrogen adsorption isotherms of Mg-IRMOF-74-III-( $\text{CH}_2\text{NH}_2$ )<sub>2</sub>-2OHBAL-Ni and Mg-IRMOF-74-III-( $\text{CH}_2\text{NH}_2$ )<sub>2</sub>-34OHBAL-Ni were measured at 77 K. The results of these measurements (Figure 5) were compared with those for Mg-MOF-74, which is the isostructural series of Mg-IRMOF-74-III-( $\text{CH}_2\text{NH}_2$ )<sub>2</sub> except 2,5-dioxido-1,4-benzenedicarboxylate was used as an organic linker. Mg-MOF-74 shows a steep hydrogen uptake at low pressure (isotherm slope as  $P \rightarrow 0$ ) indicating strong interactions between H<sub>2</sub> molecules and the framework.<sup>11</sup> In contrast, Mg-IRMOF-74-III-( $\text{CH}_2\text{NH}_2$ )<sub>2</sub>-2OHBAL-Ni and Mg-IRMOF-74-III-( $\text{CH}_2\text{NH}_2$ )<sub>2</sub>-34OHBAL-Ni do not show such steep hydrogen uptake at low pressures. We hypothesize that the post-synthetically-installed ligands interact strongly with the frameworks' open metal sites, deactivating their interactions with hydrogen. This is evidenced by the dramatic decrease in CO<sub>2</sub> uptake capacities measured for the materials at 298 K, where no steep uptake is also observed, as is typical for such materials [11].

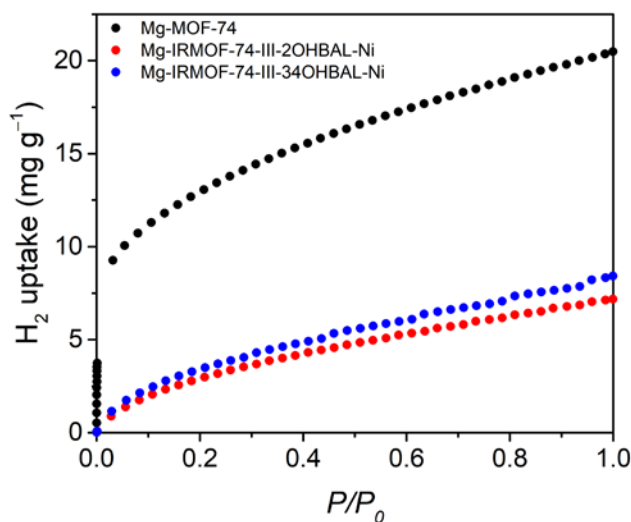


Figure 5. Comparison of low-pressure hydrogen adsorption isotherms at 77 K of Mg-MOF-74, Mg-IRMOF-74-III-2OHBAL-Ni, and Mg-IRMOF-74-III-34OHBAL-Ni



## CONCLUSIONS AND UPCOMING ACTIVITIES

As was previously discussed, Mg-IRMOF-74-III analogs were synthesized, characterized, and post-synthetically modified to incorporate Ni(II) complexes. These materials did not meet the targeted goals of the project with respect to gravimetric and volumetric hydrogen adsorption capacity. Therefore, experiments designed to evaluate the materials' lifetimes, onboard efficiencies, fill times, and minimum full flow rates were not conducted. At this time, no additional work is currently funded. However, the remaining open issues could be addressed via the synthesis of and subsequent analogous experimentation on an expanded framework such as Mg-IRMOF-74-V. In this material, it is likely that the distances between the post-synthetically-installed ligands and the framework-based open metal sites will be sufficiently large as to prevent strong interactions. Should this be the case, the Mg-IRMOF-74-V analogue would exhibit higher hydrogen adsorption capacities than either Mg-IRMOF-74-III-(CH<sub>2</sub>NH<sub>2</sub>)<sub>2</sub>-2OHBAL-Ni or Mg-IRMOF-74-III-(CH<sub>2</sub>NH<sub>2</sub>)<sub>2</sub>-34OHBAL-Ni and would warrant additional study and potential implementation.

## REFERENCES

1. H. Furukawa, K.E. Cordova, M. O'Keeffe, and O.M. Yaghi, "The Chemistry and Applications of Metal-Organic Frameworks," *Science* 341 (2013): 1230444.
2. J.L. Rowsell, A.R. Millward, K.S. Park, and O.M. Yaghi, "Hydrogen Sorption in Functionalized Metal-Organic Frameworks," *Journal of the American Chemical Society* 126 (2004): 5666-5667.
3. A.G. Wong-Foy, A.J. Matzger, and O.M. Yaghi, "Exceptional H<sub>2</sub> Saturation Uptake in Microporous Metal-Organic Frameworks," *Journal of the American Chemical Society* 128 (2006): 3494-3495.
4. S.S. Kaye, A. Dailly, O.M. Yaghi, and J.R. Long, "Impact of Preparation and Handling on the Hydrogen Storage Properties of Zn<sub>4</sub>O(1,4-benzenedicarboxylate)<sub>3</sub> (MOF-5)," *Journal of the American Chemical Society* 129 (2007): 14176-14177.
5. J.L. Rowsell and O.M. Yaghi, "Effects of Functionalization, Catenation, and Variation of the Metal Oxide and Organic Linking Units on the Low-Pressure Hydrogen Adsorption Properties of Metal-Organic Frameworks," *Journal of the American Chemical Society* 128 (2006): 1304-1315.
6. B. Chen, M. Eddaoudi, T. Reineke, J. Kampf, M. O'Keeffe, and O. Yaghi, "Cu<sub>2</sub>(ATC)·6H<sub>2</sub>O: Design of Open Metal Sites in Porous Metal-Organic Crystals (ATC: 1,3,5,7-Adamantane Tetracarboxylate)," *Journal of the American Chemical Society* 122 (2000): 11559-11560.
7. W. Zhou, H. Wu, and T. Yildirim, 2008. "Enhanced H<sub>2</sub> Adsorption in Isostructural Metal-Organic Frameworks with Open Metal Sites: Strong Dependence of the Binding Strength on Metal Ions," *Journal of the American Chemical Society* 130 (2008): 15268-15269.
8. M.T. Kapelewski, S.J. Geier, M.R. Hudson, D. Stück, J.A. Mason, J.N. Nelson, D.J. Xiao, Z. Hulvey, E. Gilmour, and S.A. FitzGerald, "M<sub>2</sub>(m-dobdc) (M = Mg, Mn, Fe, Co, Ni) Metal-Organic Frameworks Exhibiting Increased Charge Density and Enhanced H<sub>2</sub> Binding at the Open Metal Sites," *Journal of the American Chemical Society* 136 (2014): 12119-12129.
9. H. Deng, S. Grunder, K.E. Cordova, C. Valente, H. Furukawa, M. Hmadeh, F. Gándara, A.C. Whalley, Z. Liu, S. Asahina, H. Kazumori, M. O'Keeffe, O. Terasaki, J.F. Stoddart, and O.M. Yaghi, "Large Pore Apertures in a Series of Metal Organic Frameworks," *Science* 336 (2012): 1018-1023.
10. A.M. Fracaroli, P. Siman, D.A. Nagib, M. Suzuki, H. Furukawa, F.D. Toste, and O.M. Yaghi, "Seven Post-synthetic Covalent Reactions in Tandem Leading to Enzyme-like Complexity within Metal-Organic Framework Crystals," *Journal of the American Chemical Society* 138 (2016): 8352-8355.
11. R.W. Flaig, T.M. Osborn Popp, A.M. Fracaroli, E.A. Kapustin, M.J. Kalmutzki, R.M. Altamimi, F. Fathieh, J.A. Reimer, and O.M. Yaghi, "The Chemistry of CO<sub>2</sub> Capture in an Amine-Functionalized Metal-Organic Framework under Dry and Humid Conditions," *Journal of the American Chemical Society* 139 (2017): 12125-12128.



12. S.M. Cohen, “Postsynthetic Methods for the Functionalization of Metal–Organic Frameworks,” *Chemical Reviews* 112 (2011): 970-1000.
13. A.D. Garnovskii, A.L. Nivorozhkin, and V.I. Minkin, “Ligand Environment and the Structure of Schiff Base Adducts and Tetracoordinated Metal-Chelates,” *Coordination Chemistry Reviews* 126 (1993): 1-69.
14. P.G. Cozzi, “Metal–Salen Schiff base complexes in catalysis: practical aspects,” *Chemical Society Reviews* 33 (2004): 410-421.
15. E. Tsivion, J.R. Long, and M. Head-Gordon, “Hydrogen Physisorption on Metal–Organic Framework Linkers and Metalated Linkers: A Computational Study of the Factors That Control Binding Strength,” *Journal of the American Chemical Society* 136 (2014): 17827-17835.
16. L.J. Wang, H. Deng, H. Furukawa, F. Gándara, K.E. Cordova, D. Peri, and O.M. Yaghi, 2014. “Synthesis and Characterization of Metal–Organic Framework-74 Containing 2, 4, 6, 8, and 10 Different Metals,” *Inorganic Chemistry* 53 (2014): 5881-5883.
17. NIST X-ray Photoelectron Spectroscopy Database, NIST Standard Reference Database Number 20, National Institute of Standards and Technology, Gaithersburg MD, 20899 (2000), doi:10.18434/T4T88K, (retrieved April 2018).
18. J. Matienzo, L.I. Yin, S.O. Grim, and W.E. Swartz Jr., “X-Ray Photoelectron Spectroscopy of Nickel Compounds,” *Inorganic Chemistry* 12 (1973): 2762-2769.